Atmospheric Environment 81 (2013) 102–111

Contents lists available at ScienceDirect

Atmospheric Environment

journal homepage: www.elsevier.com/locate/atmosenv

The observed response of Ozone Monitoring Instrument (OMI) NO_2 columns to NO_x emission controls on power plants in the United States: 2005–2011☆

Bryan N. Duncan [a, *], Yasuko Yoshida [a, b], Benjamin de Foy [c], Lok N. Lamsal [a, d], David G. Streets [e], Zifeng Lu [e], Kenneth E. Pickering [a], Nickolay A. Krotkov [a]

[a] Atmospheric Chemistry and Dynamics Laboratory, NASA Goddard Space Flight Center, Greenbelt, MD, USA
[b] Science Systems and Applications, Inc., Lanham, MD, USA
[c] Saint Louis University, St. Louis, MO, USA
[d] Goddard Earth Sciences Technology & Research, Universities Space Research Association, Columbia, MD, USA
[e] Argonne National Laboratory, Argonne, IL, USA

HIGHLIGHTS

- Satellite data may be used to monitor changes in NO_x emissions from power plants.
- The changes in NO_x emissions and NO_2 columns are well correlated.
- Significant changes in regional NO_2 levels influence the signal of the facilities.
- We discuss factors that affect the detection of NO_2 from power plants.

ARTICLE INFO

Article history:
Received 26 June 2013
Received in revised form
28 August 2013
Accepted 31 August 2013

Keywords:
Ozone Monitoring Instrument
Nitrogen dioxide
Air quality
Space-based observations
Power plant emissions
Emission control devices

ABSTRACT

We show that Aura Ozone Monitoring Instrument (OMI) nitrogen dioxide (NO_2) tropospheric column data may be used to assess changes of the emissions of nitrogen oxides (NO_x) from power plants in the United States, though careful interpretation of the data is necessary. There is a clear response for OMI NO_2 data to NO_x emission reductions from power plants associated with the implementation of mandated emission control devices (ECDs) over the OMI record (2005–2011). This response is scalar for all intents and purposes, whether the reduction is rapid or incremental over several years. However, it is variable among the power plants, even for those with the greatest absolute decrease in emissions. We document the primary causes of this variability, presenting case examples for specific power plants.

Published by Elsevier Ltd.

1. Introduction

In response to federal and state regulations, total emissions of nitrogen oxides ($NO_x = NO + NO_2$) decreased since the late 1990s by 47% in the United States (US). Emissions from electric power generation and highway vehicles, two of the largest sources, decreased by 68% and 43%, respectively (http://www.epa.gov/ttn/chief/trends/index.html). The US Environmental Protection Agency (EPA) issued the 1998 NO_x State Implementation Plan (SIP) Call with the intent to reduce emissions in 22 eastern states during the summer season so as to decrease ozone. In 2005, it issued the Clean Air Interstate Rule (CAIR) for 27 eastern states with the goal to decrease NO_x emissions even further from power plants. Individual state rules and court orders have also contributed to power plant emission reductions. The mobile source of NO_x emissions has declined nationwide as a result of the requirements of the Clean Air Act Amendments (CAAA) of 1990, specifically the Tier 1 (phased-in between 1994 and 1997) and more stringent Tier 2 (phased-in

* Corresponding author. Code 614 NASA Goddard Space Flight Center, Greenbelt, MD 20771, USA. Tel.: +1 301 614 5994; fax: +1 301 614 5903.
E-mail address: Bryan.N.Duncan@nasa.gov (B.N. Duncan).

1352-2310/$ – see front matter Published by Elsevier Ltd.
http://dx.doi.org/10.1016/j.atmosenv.2013.08.068

between 2004 and 2009) standards, and the gradual turnover of the fleet of light-duty vehicles (e.g., Dallmann and Harley, 2010; McDonald et al., 2012).

Satellite observations confirm that NO_2 columns over power plants and urban areas in the US have declined as a result. Kim et al. (2006) used both the European Remote-sensing Satellite-2 (ERS-2) Global Ozone Monitoring Experiment (GOME) and Envisat SCanning Imaging Absorption spectroMeter for Atmospheric CHartographY (SCIAMACHY) NO_2 column data to infer that NO_x emissions from power plants in the Ohio River Valley decreased from 1997 to 2005 by about 35%, which is consistent with reported emission changes from the Continuous Emissions Monitoring System (CEMS). Kim et al. (2009) were the first to show that NO_2 columns from a model of chemistry and transport (CTM) using CEMS data were consistent with columns from three retrievals (i.e., the University of Bremen Ozone Monitoring Instrument (OMI), National Aeronautics and Space Administration (NASA) OMI operational product, and SCIAMACHY) over 13 isolated power plants in the western US in 2005. Russell et al. (2012) used NO_2 column data from the OMI Berkeley High Resolution (BEHR) retrieval algorithm to infer that NO_x emissions changes from large power plants were variable because of regionally-specific regulations, decreasing by $26 \pm 12\%$ from 2005 to 2011. They estimated an average total reduction of $32 \pm 7\%$ in NO_2 for US cities from 2005 to 2011 with a 34% decrease in NO_2 from mobile sources. They attributed part of the observed decline to the turnover in the mobile source fleet and part to the global economic recession that began in 2008.

To comply with federal and state requirements, emission control devices (ECDs) were installed on power plants, which create a natural experiment to assess the response of the satellite-observed tropospheric NO_2 column to a known, and oftentimes rapid and significant, change in a power plant's emissions. For instance, in Selective Catalytic Reduction systems (SCRs), ammonia is mixed with the flue gas before entering the reactor so that ammonia and NO_x react to form nitrogen and water. Other techniques to reduce NO_x emissions include the installation of Low NO_x Burners (LNBs) and Rotating Opposed Fire Air (ROFA) devices, which may be used in combination with SCRs. ECDs remove up to 90% of NO_x from the effluent.

The purpose of this study is to use Aura OMI data (2005–2011) to understand the response of the NO_2 column to a change in a power plant's emissions; hereafter, we refer to this as the "Response". As we will show, the Response is scalar, as the change in the column is a linear function of the change in emissions for all intents and purposes. However, there are variations in the magnitudes of the Responses. We document the primary sources of these variations. Quantifying the Response and understanding the primary drivers of its variability for power plants in the US will allow for 1) confidence in the assessment of the impact of ECDs on air quality and 2) better estimation of NO_x emissions from large point sources in other regions of the world where estimates of emissions are often highly uncertain.

2. Data and method

2.1. OMI NO_2 column data

The OMI is on board the Aura satellite, which was launched on July 15, 2004 into a sun-synchronous polar orbit. It measures direct and backscattered solar radiation in the UV–visible range from 264 to 504 nm (Levelt et al., 2006) and provides early afternoon (local time 1300–1430) NO_2 columns at a spatial resolution of up to 13×24 km^2 with global coverage within two days. We use the OMI operational tropospheric NO_2 column data product (version 2.1, collection 3) from 2005 to 2011, which is available from the NASA Goddard Earth Sciences, Data and Information Services Center (GES DISC; http://disc.sci.gsfc.nasa.gov). The early releases of the two main OMI products of NO_2, one from NASA and the other from the Royal Netherlands Meteorological Institute (KNMI), showed large differences for some regions (Lamsal et al., 2010). This current version represents substantial OMI retrieval algorithm improvements (Boersma et al., 2011; Bucsela et al., 2013, and references therein) from its preceding version 1.0, so that it is now feasible to derive quantitative information about NO_x emissions from large point sources (Streets et al., 2013). The current, refined retrieval algorithms of both research groups, though different in their approaches, now produce very similar columns.

Retrieval of tropospheric NO_2 columns involves (1) retrieval of NO_2 abundance along the viewing path (slant column) with a Differential Optical Absorption Spectroscopy (DOAS) fit (Platt, 1994) in the 405–465 nm wavelength range, (2) computation of an air mass factor (AMF) by integrating the relative vertical distribution (shape factors) of NO_2 weighted by altitude-dependent scattering weights for NO_2 (Palmer et al., 2001), (3) removal of cross-track artifacts (stripes) resulting from insufficient calibration in the OMI backscattered reflectances, and (4) separation of stratospheric and tropospheric NO_2 components (Bucsela et al., 2013).

The tropospheric AMF is sensitive to the a priori NO_2 profile shape. The retrieval of the operational NO_2 product uses NO_2 shape factors generated from the NASA Global Modeling Initiative (GMI; http://gmi.gsfc.nasa.gov/) CTM at 2.5° longitude × 2° latitude resolution grids. In this work, we use the NO_2 product discussed in Lamsal et al. (2013) that was generated with high resolution (0.67° longitude × 0.5° latitude) over the US. NO_2 shape factors were derived from a nested-grid GEOS-Chem CTM (http://acmg.seas.harvard.edu/geos/) simulation and scattering weights for NO_2. Use of NO_2 shape factors from the nested simulation improves the representation of vertical distributions, including those of the elevated plumes of power plants (Lamsal et al., 2013). The errors in the individual pixel tropospheric NO_2 columns under clear-sky conditions are estimated to be 30% (Boersma et al., 2004).

The OMI tropospheric NO_2 columns agree with in situ and ground-based measurements within 20% (Lamsal et al., 2013; Bucsela et al., 2013). Individual clear-sky (i.e., cloud fraction < 0.3) data not affected by the so called "row anomaly" (Dobber and Braak, 2010) were allocated by area-weights into 0.1° longitude × 0.1° latitude grids. The row anomaly is the result of a partial blockage of the field of view of the OMI, which lengthens the time necessary to obtain global coverage from one day to two days. For consistency over the OMI record, we restricted our analysis to scan positions 10–23 as they are unaffected by the row anomaly.

There are rarely ideal conditions for assessing emissions changes from power plants from space, so we used all available data, regardless of season. Lu and Streets (2012), and references therein, recommend using data only for summer (e.g., the policy-relevant ozone season of May–September) for a variety of reasons. For instance, the chemical lifetime of NO_x tends to be shortest in summer, which has the advantage that a facility's emissions are convolved less with NO_x from other sources than in other seasons. However, there are disadvantages to using data only for the ozone season, such as the stratospheric contribution to the total NO_2 column, and the associated error, is seasonally greatest and important.

For the purposes of this study, it was not practical to restrict our analysis to the ozone season as many facilities, including some of the largest emitters, were already operating ECDs during the ozone season at the start of our study period, especially in the eastern US. In Section 3, we show that the relationship between a facility's NO_x emissions and the OMI NO_2 column over the power plant is much stronger in the southern US than in the northern US, where the

seasonal variation in the chemical lifetime of NO_x is more pronounced. We discuss the implications of using all available data in Section 3.2.5.

2.2. Selection of power plants

We identified the top 100 highest-emitting power plants in 2005 based on the US national NO_x emissions inventory (http://www.epa.gov/ttn/chief/eiinformation.html). If there is more than one power plant within a 0.4° longitude × 0.4° latitude gridbox, we combined and treated them as one facility. Then, we used the Emission Database for Global Atmospheric Research version 4 (EDGAR v4; http://edgar.jrc.ec.europa.eu/), which is for 2005 and is available on a 0.1° longitude × 0.1° latitude resolution grid, to select the power plants least affected by other industrial sources within a 0.4° longitude × 0.4° latitude area around the facility. Lu and Streets (2012) found that the agreement between NO_2 columns and NO_x emissions improves with increasing relative contribution of the power plant's emissions to total NO_x emissions from all sources within a NO_2 column gridbox; they refer to this quantity as f_{power}. For this study, we required that $f_{power} > 0.90$, which eliminated 45 of the top 100 highest-emitting power plants from our analysis. The locations of the facilities used in this analysis are shown in Fig. 1. Information for each power plant is given in Table 1.

The characteristics of a plume from a power plant depend on variations in meteorology (e.g., "plume meandering"; Beirle et al., 2011) and chemistry, so we used the maximum value of the plume for each overpass whether in the gridbox containing the facility or in adjacent gridboxes (i.e., a 0.3° longitude × 0.3° latitude area) to create monthly averages. We found that the correlation between the change in emissions from a power plant and the concomitant change in the OMI NO_2 column is best for this fine grid resolution (i.e., 0.1° longitude × 0.1° latitude) as compared to more coarse resolutions (e.g., 0.25° longitude × 0.25° latitude).

2.3. Definition of the response (ρ)

In order to reflect the relative contributions of NO_x emissions from a power plant to the total NO_x emissions (and column), we define the following parameters: E^T, E^{PP}, and E^O, which represent NO_x emissions from all sources within a gridbox, the power plant, and sources other than the power plant, respectively, where $E^T = E^{PP} + E^O$. Similarly, NO_2^T, NO_2^{PP} and NO_2^O represent, respectively, the total NO_2 column within a gridbox, the portion of the column associated with the power plant, and the portion of the column associated with all other sources, including NO_2 advected into the gridbox, where $NO_2^T = NO_2^{PP} + NO_2^O$.

As defined in the introduction, the Response (ρ) is given by:

$$\rho = \Delta NO_2^{PP}/\Delta E^{PP} = \left(\Delta NO_2^T - \Delta NO_2^O\right) \Big/ \left(\Delta E^T - \Delta E^O\right) \quad (1)$$

where Δ represents the change in NO_2 column or NO_x emissions. Rearranging Equation (1) into linear form:

$$\Delta NO_2^T = \rho^* \left(\Delta E^T - \Delta E^O\right) + \Delta NO_2^O \quad (2)$$

where ρ is the slope of the line and ΔNO_2^O is the y-intercept. In the ideal situation where ΔE^O and ΔNO_2^O equal zero, Equation (2) simplifies to:

$$\Delta NO_2^T = \rho^* \Delta E^{PP} \quad (3)$$

In this case, ΔNO_2^T, such as determined from OMI data, is solely due to ΔE^{PP}. ΔE^{PP} in all figures and Table 1 in this manuscript is the sum of emissions for those days where OMI data are available. Consequently, ΔE^{PP} is less than the total change in a facility's emissions over a given time period.

Though Equations (1)–(3) are rather straightforward, ρ is a complicated parameter that is a function of the chemical lifetime of NO_x, meteorology, and the factors that affect the partitioning of NO_x into NO and NO_2 (e.g., Martin et al., 2003; Stavrakou et al., 2008; Beirle et al., 2011; Lamsal et al., 2011; Walter et al., 2012; Zhou et al., 2012). The dependence of ρ on these factors is discussed in the Supplemental Material. Accounting for the complexities of ρ requires a CTM, ideally with a plume-in-grid technique, to properly treat the evolution of a power plant's plume. In Section 3, we show that this onerous step is not necessary for our practical application, particularly given the large uncertainties associated with the OMI data discussed in Sections 2.1 and 3.2. In practice, ρ is relatively stable

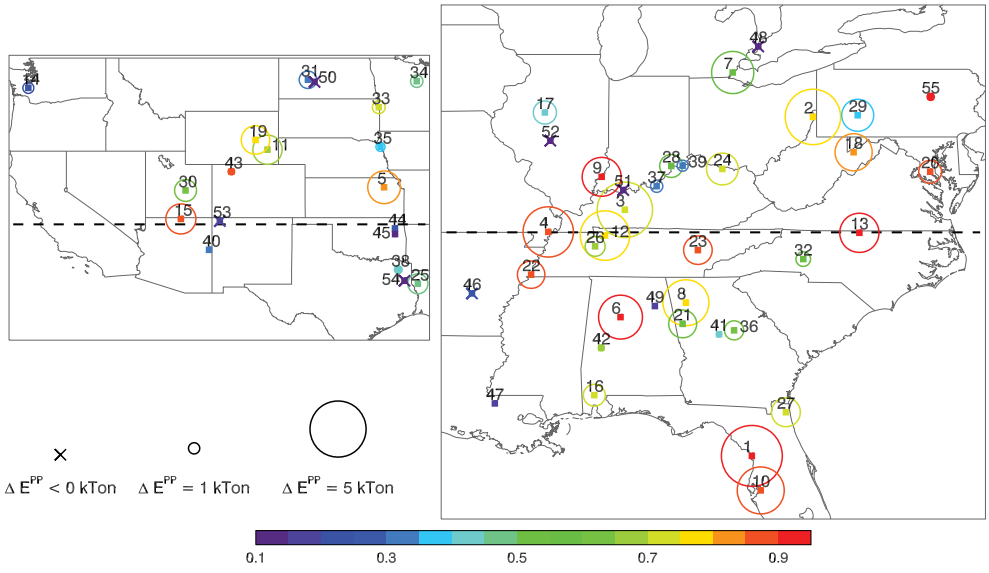

Fig. 1. The locations of the facilities listed in Table 1 with the facility identifier beside each point. The magnitude of ΔE^{PP} (kTon) is indicated by the size of the circle around the square indicating the facility location. The color of each square corresponds to the correlation (r^2) shown in Table 1. The horizontal dashed line indicates 36.5°N latitude, which is the boundary between the southern and northern US in Fig. 3. (For interpretation of the references to color in this figure legend, the reader is referred to the web version of this article.)

Table 1
Information for individual power plants.

ID	Facility name	State	Lati-tude	Long-itude	ΔE^{PP} (kTon)	ΔE^{PP} (%)	ΔNO_2^T ($\times 10^{15}$ molec cm^{-2})	ΔNO_2^T (%)	ρ ($\times 10^{15}$ molec (cm^2 kTon)$^{-1}$)	r^2	Std Err	$N < 3$
1	Crystal River	FL	29.0	−82.7	5.4	69.5	1.5	36.6	0.28	0.91	0.23	0
2	Cardinal + WH Sammis	OH	40.4	−80.6	4.9	69.9	2.6	35.5	0.44	0.77	0.70	15
3	Paradise	KY	37.3	−87.0	4.9	69.0	2.0	36.1	0.31	0.71	0.58	2
4	NewMadrid	MO	36.5	−89.6	4.5	74.7	1.1	26.5	0.24	0.85	0.26	2
5	Jeffrey EC	KS	39.3	−96.1	2.9	44.3	0.4	11.4	0.12	0.82	0.23	2
6	Gorgas + James H. Miller Jr.	AL	33.6	−87.1	3.9	49.9	1.3	28.1	0.34	0.91	0.29	2
7	Monroe	MI	41.9	−83.3	3.8	59.7	2.0	23.4	0.48	0.58	0.83	14
8	Bowen	GA	34.1	−84.9	4.1	69.8	1.8	30.2	0.35	0.75	0.40	0
9	Gibson	IN	38.4	−87.8	3.5	56.5	0.9	17.5	0.23	0.90	0.40	2
10	Big Bend	FL	27.8	−82.4	4.2*	76.7	2.3	40.9	0.53	0.89	0.31	0
11	Laramie River	WY	42.1	−104.9	2.6	41.8	0.5	19.7	0.14	0.66	0.17	2
12	Cumberland	TN	36.4	−87.7	4.4	79.3	1.3	30.7	0.23	0.75	0.32	0
13	Roxboro	NC	36.5	−79.1	3.5	67.2	1.5	29.8	0.38	0.92	0.40	0
14	Centralia	WA	46.8	−122.9	1.0*	33.4	0.6	12.7	0.23	0.24	0.40	13
15	Navajo	AZ	36.9	−111.4	2.7	28.5	0.9	24.1	0.26	0.88	0.23	0
16	Barry	AL	31.0	−88.0	2.0	49.3	0.5	15.6	0.26	0.74	0.17	0
17	Powerton	IL	40.5	−89.7	2.1	41.3	0.9	19.3	0.21	0.44	0.36	9
18	Mount Storm	WV	39.2	−79.3	3.3	81.4	1.6	33.4	0.41	0.83	0.51	3
19	Dave Johnston	WY	42.8	−105.8	2.5	62.3	0.5	24.3	0.21	0.76	0.13	8
20	Chalk Point	MD	38.5	−76.7	2.0*	61.0	2.6	32.5	1.08	0.89	0.66	0
21	Wansley	GA	33.4	−85.0	2.5	78.3	1.2	22.6	0.37	0.54	0.33	0
22	Allen Fossil	TN	35.1	−90.1	2.4	82.1	1.0	20.0	0.43	0.88	0.35	0
23	Kingston	TN	35.9	−84.5	2.5	87.6	1.1	24.9	0.47	0.86	0.41	11
24	JM Stuart	OH	38.6	−83.7	2.8	66.0	2.2	35.4	0.62	0.73	0.64	6
25	Dolet Hills	LA	32.0	−93.6	1.8*	58.0	0.1	2.8	0.14	0.47	0.17	3
26	Johnsonville	TN	36.0	−88.0	1.8*	45.5	1.2	27.0	0.51	0.66	0.31	0
27	St. Johns River	FL	30.4	−81.6	2.6	60.5	1.9	34.6	0.53	0.73	0.31	0
28	Clifty Creek	IN	38.7	−85.4	2.1	53.4	1.9	30.5	0.65	0.57	0.60	4
29	Conemaugh + Homer City	PA	40.4	−79.1	2.9	37.1	2.1	27.2	0.49	0.39	0.78	10
30	Hunter	UT	39.0	−111.0	2.0	38.2	0.5	14.6	0.21	0.60	0.37	7
31	Antelope Valley	ND	47.4	−101.8	1.6*	44.0	0.1	4.8	0.16	0.32	0.19	15
32	Marshall	NC	35.6	−81.0	1.3*	35.5	1.6	26.5	0.79	0.59	0.39	0
33	Big Stone	SD	45.3	−96.5	1.1*	39.2	0.3	11.5	0.21	0.73	0.18	23
34	Boswell	MN	47.3	−93.7	1.1*	50.4	0.1	6.4	0.15	0.45	0.19	22
35	George Neal North	IA	42.3	−96.4	0.8*	31.3	0.2	7.7	0.32	0.39	0.22	11
36	Harllee Branch	GA	33.2	−83.3	1.7*	35.2	1.1	25.0	0.38	0.61	0.27	0
37	Mill Creek	KY	38.1	−85.9	1.1*	40.5	0.8	12.9	0.49	0.30	0.50	0
38	Monticello	TX	33.1	−95.0	0.7*	20.0	0.4	11.2	0.56	0.44	0.23	0
39	Ghent	KY	38.7	−85.0	1.0*	39.6	1.8	27.4	0.80	0.31	0.57	2
40	Coronado	AZ	34.6	−109.3	0.3*	10.1	0.2	9.3	0.18	0.34	0.15	0
41	Scherer	GA	33.1	−83.8	0.5*	10.9	1.0	22.0	0.84	0.43	0.31	0
42	Greene County	AL	32.6	−87.8	0.5*	28.4	0.4	13.8	0.65	0.65	0.16	0
43	Craig	CO	40.5	−107.6	0.6*	22.3	0.6	25.0	0.86	0.89	0.25	30
44	Grand River Dam	OK	36.2	−95.3	0.3*	8.4	0.6	14.3	0.34	0.26	0.25	0
45	Muskogee	OK	35.8	−95.3	0.4*	9.4	0.6	17.3	0.17	0.10	0.23	0
46	White Bluff	AR	34.4	−92.1	−0.2*	−3.9	0.0	0.5	0.24	0.22	0.21	1
47	Big Cajun2	LA	30.7	−91.4	0.1*	2.3	0.3	6.7	0.51	0.16	0.25	0
48	Belle River + St. Clair	MI	42.8	−82.5	−0.1*	−4.6	1.1	17.5	−0.07	0.00	0.61	21
49	Gadsden	AL	34.0	−86.0	0.2*	42.1	0.6	16.5	0.74	0.16	0.21	0
50	LelandOlds + MiltonRYoung	ND	47.2	−101.3	−0.5*	−10.4	0.8	21.9	−0.21	0.15	0.24	20
51	Rockport	IN	37.9	−87.0	−0.1*	−2.9	1.8	27.7	−0.91	0.11	0.42	4
52	Kincaid	IL	39.6	−89.5	−0.6*	−26.3	0.8	21.2	0.00	0.00	0.35	4
53	Four Corners + San Juan	NM	36.7	−108.5	0.0*	−0.3	1.0	15.0	−0.19	0.18	0.45	2
54	Martin Lake	TX	32.3	−94.6	−0.7*	−19.4	0.3	8.6	−0.22	0.06	0.24	0
55	Montour	PA	41.1	−76.7	0.6*	25.6	0.8	14.4	1.04	0.94	0.66	10

ΔE^{PP} and ΔNO_2^T are calculated as the mean of 2005 and 2006 minus the mean of 2010 and 2011; the total sum of emissions includes only those days where OMI data are available so that ΔE^{PP} is less than the total change in a facility's emissions over a given time period.
ρ is the slope of the line fit to annual mean OMI data and annual total CEMS data in Fig. 2 and S1 (right column); alternately, one could define ρ as the change in NO_2^T and E^{PP} between two specific years, such as 2005 and 2011, which gives a similar value for ρ as the slope of a linear fit to the data when ΔE^{PP} is large.
r^2 is the correlation of annual mean OMI data and annual total CEMS data (Fig. 2 and S1; right column).
StdErr is the standard error of the mean of NO_2^T.
$N < 3$ is the number of months between 2005 and 2011 which have less than three days to create the monthly average.
We indicate those facilities where the regional background is large relative to the signal of the facility with an "*" in the column containing ΔE^{PP}. Our criteria for this determination is ΔE^{PP} <2 kTon (see Fig. 6) and/or location within regionally polluted areas.

for each site so that ΔNO_2^T can be treated as linearly proportional to ΔE^T (e.g., Martin et al., 2003; Kaynak et al., 2009; Kim et al., 2009).

3. Results

Over the Aura record, 2005–2011, NO_x emissions from electric power generation decreased by 48% in the US (http://www.epa.gov/ttn/chief/trends/index.html). The CEMS data indicate that there was a large (>50%) decrease between 2005 and 2011 in annual emissions at 22 power plants that we include in our study (Table 1), presumably because of the implementation of new ECDs. Emissions at most of the facilities decreased by >20%, while emissions at seven facilities did not change or increased. At many facilities, emissions decreased rapidly, but they decreased

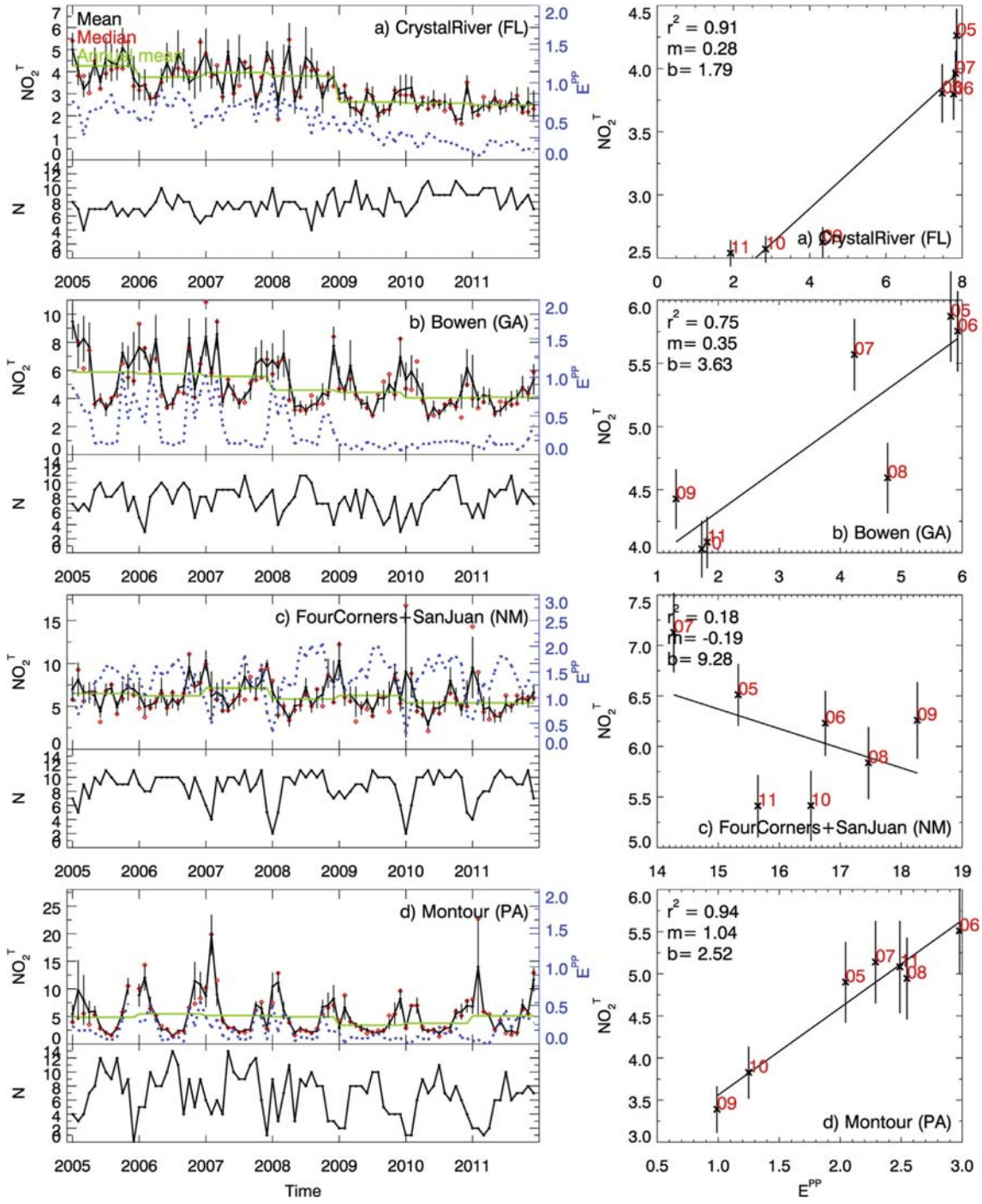

Fig. 2. (left) Monthly mean NO_2^T (black line; $\times 10^{15}$ molecules cm^{-2}) and E^{PP} (blue dotted line; kTon) data from 2005 to 2011 for four power plants. Vertical black lines represent the standard error of the mean of the OMI data. The sample size (N) is the number of days with data used to create monthly means. The annual mean NO_2^T data are represented with a green line and the monthly median data as an open red diamond. (right) Annual mean NO_2^T ($\times 10^{15}$ molecules cm^{-2}) versus annual E^{PP} (kTon) data. The red numbers represent the years that correspond to the annual means (e.g., "09" = 2009). The correlation (r^2) of the data is shown along with the slope (m) and *y*-intercept (b) of a line fit to the data. m is ρ as shown in Table 1. (For interpretation of the references to color in this figure legend, the reader is referred to the web version of this article.)

incrementally at others, which we know to be associated with, for instance, the implementation over time of ECDs on specific units within a facility.

3.1. Response of OMI NO_2 to the implementation of ECDs

Fig. 2 (left column) shows monthly total E^{PP} and monthly mean NO_2^T for several facilities over the OMI record (Figure S1 shows this information for all facilities listed in Table 1.). The Crystal River facility (ID #1; Fig. 2a) in Florida had the largest ΔE^{PP} (70%; Table 1). The CEMS data show that emissions began decreasing rapidly during the installation of ECDs that came online in June 2009 (Unit 5) and May 2010 (Unit 4). There were concomitant decreases in NO_2^T with a 37% overall reduction (Table 1). The correlation of the annually mean NO_2^T and annual total E^{PP} (Fig. 2, right column) is high ($r^2 = 0.91$). ρ (i.e., the slope

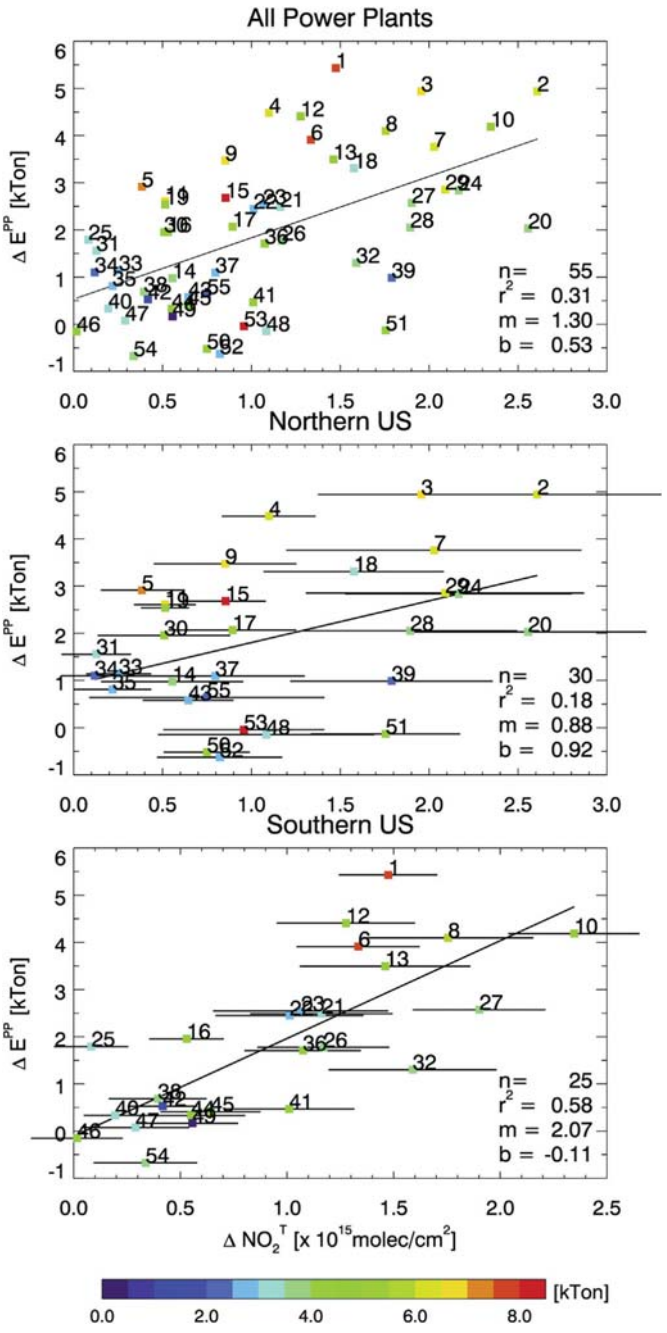

Fig. 3. (top) ΔE^{PP} (kTon) as compared to ΔNO_2^T ($\times 10^{15}$ molecules cm^{-2}) as the mean of 2005 and 2006 minus the mean of 2010 and 2011 (Table 1). The colored dots indicate the magnitude of the mean E^{PP} of 2005 and 2006. The number associated with each point corresponds to a particular power plant identified in Table 1. *n* is sample size (i.e., the number of power plants) used in the correlation statistic (r) and line fit, where m is the slope and b is the *y*-intercept. (middle) The same as (top), but for only those facilities at latitudes >36.5°N. The horizontal lines represent the standard error of the means of the OMI data. (bottom) The same as (middle), but for only those facilities at latitudes <36.5°N.

(m) of the line in Fig. 2 and S1; right column) at the Crystal River facility is 0.28.

ρ at the Bowen facility (ID #8) in Georgia is similar (0.35) to the Crystal River facility, though the correlation is somewhat lower ($r^2 = 0.75$; Fig. 2b). ECDs were operated at Bowen during the ozone season through 2008, but year-round afterward (Fig. 2b; left column). Overall, E^{PP} decreased by 70% from 2005 to 2011 with a corresponding decrease in NO_2^T of 30%. Although this facility is generally upwind of the Atlanta metropolitan area, the NO_2 column is likely influenced to some degree by this urban source, depending on meteorology and season, which may explain the scatter in E^{PP} and NO_2^T in Fig. 2b (right column). Nevertheless, the impact of year-round ECDs on NO_2^T is clear from the beginning of 2009.

We found that ρ's are <1 at all but two of the facilities (Table 1). There is a wide range of values, but there is no clustering, such as with latitude. In the next section, we discuss sources of variation of ρ among the facilities.

3.2. Sources of variation in the response

Fig. 3 shows ΔE^{PP} and ΔNO_2^T (Table 1) for all power plants. Overall, the correlation ($r^2 = 0.31$) is weak and does not improve much when only facilities are considered where $E^{PP} > 4$ kTon in 2005. The poor correlation occurs whether the absolute or relative changes are considered. The correlation for the facilities in the southern US is better ($r^2 = 0.58$; $n = 25$) than in the northern US ($r^2 = 0.18$; $n = 30$; Fig. 3), though it is important to note that ρ's at most individual facilities are generally scalar, including in the northern US (Figure S1) (There are too few facilities in the western US with which to draw any conclusion about a possible systematic bias between eastern and western facilities.). We chose 36.5°N latitude (shown in Fig. 1) to separate the northern and southern US as the range of the standard error of the means of the OMI data for the individual facilities is 0.1–0.4 below this latitude and 0.1–0.8 above this latitude (Fig. 3; Table 1). In the following subsections, we discuss the sources of variation of ρ for the power plants, including those that cause the differences between facilities in the northern and southern US.

3.2.1. Magnitude of emissions reduction

For most facilities, we found that ρ is scalar for all intents and purposes and ΔNO_2^T is well correlated with ΔE^{PP} given that ΔE^{PP} was large (Fig. 1; Table 1), which is consistent with the findings of Lu and Streets (2012). The correlations (r^2) between annual NO_2^T and E^{PP} (Table 1) are >0.5 at 32 of the 55 facilities and, not surprisingly, rise linearly with increasing ΔE^{PP}, which will be discussed further in Section 3.2.6.

As with all satellite data, it is important to consider the issue of the signal-to-noise ratio (SNR). For our purposes, this means that the SNR increases with the magnitude of E^{PP}. Some of the facilities in Table 1 had relatively small annual emissions in 2005 so that meteorological variations and large changes in regional NO_2 levels, for instance, may obscure their ρ's. Not all the power plants in our study used ECDs and some had relatively small variations in annual emissions. We included these facilities to help us understand what factors influence ρ.

3.2.2. Retrieval issues

Errors are introduced into the retrieval during the conversion of the measured OMI slant column to a more useful vertical column using a tropospheric AMF, a complex function of information on a priori NO_2 profile shapes, surface albedo, clouds, aerosols (not implicitly accounted for), etc. (e.g., Boersma et al., 2011). The use of coarsely-resolved retrieval parameters (e.g., NO_2 profile shapes, surface albedo) could introduce large errors in retrievals at places where these parameters have large spatial variability (Zhou et al., 2009; Boersma et al., 2011), such as in mountainous and desert areas in the western US. For example, the emissions remained relatively stable over our study period at the Four Corners/San Juan facility (ID #53) in New Mexico, the facility with one of the highest annual emissions (Fig. 2c). Though new ECDs were not installed, the year-to-year variation in E^{PP} was larger at this facility than ΔE^{PP}

for some smaller facilities that implemented ECDs. However, the correlation ($r^2 = 0.18$) associated with ρ is weak, which may result from the parameters used in the AMF as the facility is located in the desert (i.e., high surface reflectivities) and near mountains characterized by variable snow cover.

3.2.3. Statistical significance

The number of individual days with OMI data (i.e., sample size (N) in Fig. 2 and S1) is typically < 10 month^{-1}, so that the standard error of the mean is oftentimes large. In these situations, the monthly average is not statistically significant. This issue is compounded for power plants at higher latitudes or elevations, such as the Big Stone (ID #33; Figure S1) facility, as OMI data are filtered for snow cover. At this facility, 23 months have <3 days of data with which to create the monthly average (Table 1), so that the annual average is weighted more heavily to spring, summer, and fall than winter. It is worth noting that the correlation of ρ ($r^2 = 0.73$) is high for this facility.

As N is not large, the monthly OMI data, as gridded for use in this study, may be skewed by outliers and bad data at all facilities. There are two winter months with obvious bad data, possibly because of improper filtering for snow and ice, at the Monroe facility (ID #7) in Michigan (Figure S1). However, the impact of this bad data is not obvious in the correlation ($r^2 = 0.58$) of ρ. Other facilities with suspect data during winter include, for instance, Gibson (ID #9), Boswell (ID #34), and Four Corners/San Juan (ID #53).

3.2.4. Proximity to urban sources

At the Big Bend facility (ID #10) near Tampa, Florida, ECDs were brought online in 2008 (Unit 3), 2009 (Unit 2), and 2010 (Unit 1), decreasing emissions by 77%. Similar to ρ (0.28) at the Crystal River facility (ID #1), which is also in Florida, ρ (0.53) at the Big Bend facility is scalar, but twice as high; NO_2^T and E^{PP} are well correlated ($r^2 = 0.89$). ΔNO_2^T at the Crystal River facility is smaller than at the Big Bend facility despite ΔE^{PP} being larger for the Crystal River facility. Due to proximity, the urban plume of Tampa influenced NO_2^T at the Big Bend facility (not shown), particularly in the earlier years of our study period. From 2005 to 2011, the OMI data indicate that NO_2^T over Tampa decreased by more than 50% ($\sim 2.5 \times 10^{15}$ molecules cm^{-2}), which, coupled with the large ΔE^{PP}, explains the larger ρ as compared to the Crystal River facility. That is, ρ for the Big Bend facility is convolved with the large decrease of NO_2 in the urban plume of Tampa (i.e., ΔNO_2^O). For facilities near large emitters, including cities, the OMI data could be filtered by wind direction to minimize the influence of these other sources.

3.2.5. Seasonal variation

The influence of the seasonal cycle in NO_2^T associated with variations in temperature and sunlight is readily apparent in Fig. 2b at the Bowen facility (ID #8) and at numerous other facilities (Figure S1). At facilities, such as Paradise (ID #3), New Madrid (ID #4), and Gibson (ID #9), the seasonal cycles in NO_2^T continue even after the ECDs were routinely used year-round. It is worth noting that the correlation of monthly NO_2^T and E^{PP} may be artificially enhanced by the coincidence of the seasonal minimum of the chemical lifetime of NO_2 in summer and the use of ECDs during the ozone season only (e.g., the Montour facility (ID #55); Fig. 2d).

As discussed in Section 2.1, we use all available data, regardless of season, to calculate ρ as many facilities operated ECDs in summer during our entire study period. The advantage of using all data is that the sample size (N) is larger, thus improving statistical significance as discussed in Section 3.2.3. Using all available OMI data will cause variation in the ρ's calculated for the facilities. The seasonal variation of the chemical lifetime is greatest at higher latitudes, which partly explains why ΔNO_2^T and ΔE^{PP} from the individual facilities are better correlated in the southern ($r^2 = 0.58$) than in the northern US ($r^2 = 0.18$; Fig. 3). However, the calculation of ρ for an individual facility should not be adversely impacted as a similar distribution of data over the course of a year is used for all years.

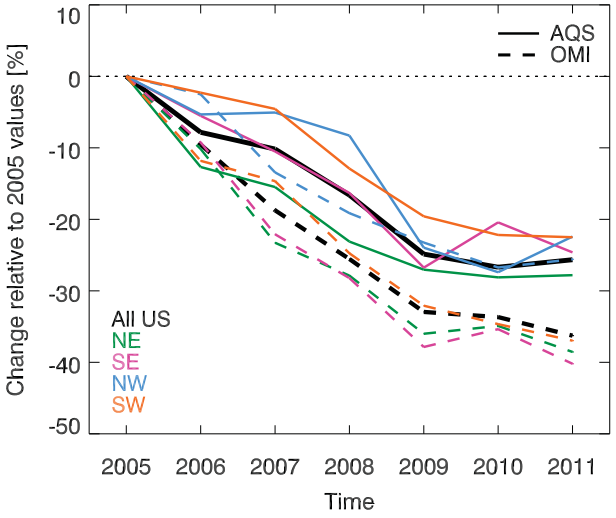

Fig. 4. Percent change of the annual mean OMI NO_2^T (dashed lines) and NO_2 from AQS surface sites (solid lines) relative to 2005 for the whole US ("All US") and four quadrants ("NE" = northeast"; "SE" = southeast; "NW" = northwest; "SW" = southwest). In total, 517 AQS sites are included. The OMI data were sampled for the 0.1° × 0.1° gridboxes in which the AQS sites lay. We used all hourly AQS data to estimate the percent change.

To understand the seasonal variability, we calculated ρ for each of the four seasons for each facility. In general, there is significant variability (>50%) in the seasonal ρ's for the typical facility, particularly ones at higher latitudes. At the Crystal River facility (ID #1) in Florida, the seasonal ρ's are similar (i.e., within ~30%), which is not surprising given the plant's southerly location. The seasonal ρ's show more variation (~50%) at the nearby Big Bend facility (ID #10), though this facility is impacted by the urban plume of Tampa as discussed in Section 3.2.4. On the other hand, there is considerably more variability in the seasonal ρ's at the Cardinal/W. H. Sammis facility (ID #2) in Ohio and the New Madrid facility (ID #4) in Missouri, which are both located at higher latitudes than the Crystal River facility and in areas with higher regional NO_2 levels.

In general, the seasonal ρ's for spring, summer and fall tend to be more similar for a typical facility with the seasonal ρ for winter being the outlier. An exception is that the seasonal ρ's for summer are less meaningful at facilities in which ECDs were used during the ozone season over the entire study period because of the low emissions and, subsequently, low SNR of the OMI data. In addition, the magnitude of NO_2^T is seasonally lowest in summer as the chemical lifetime is seasonally shortest. One would expect that seasonal ρ's for spring and fall are similar at a given facility because of the similar chemical lifetimes in these two seasons. Generally, this is the case, particularly for the high-emitting facilities.

The seasonal ρ's for winter tend to show considerable variability because of the latitudinal-dependence of the seasonal variation of the chemical lifetime and because of missing data as discussed in Section 3.2.3. In addition, the regional NO_2 levels are seasonally highest in winter because the chemical lifetime is seasonally longest, so that the ratio of NO_2 from the power plant relative to the regional level is seasonally lowest at many facilities.

The methodology that we present in this manuscript to assess the impact of the implementation of an ECD on the NO_2 level above a facility may be tailored for specific applications. For instance, one

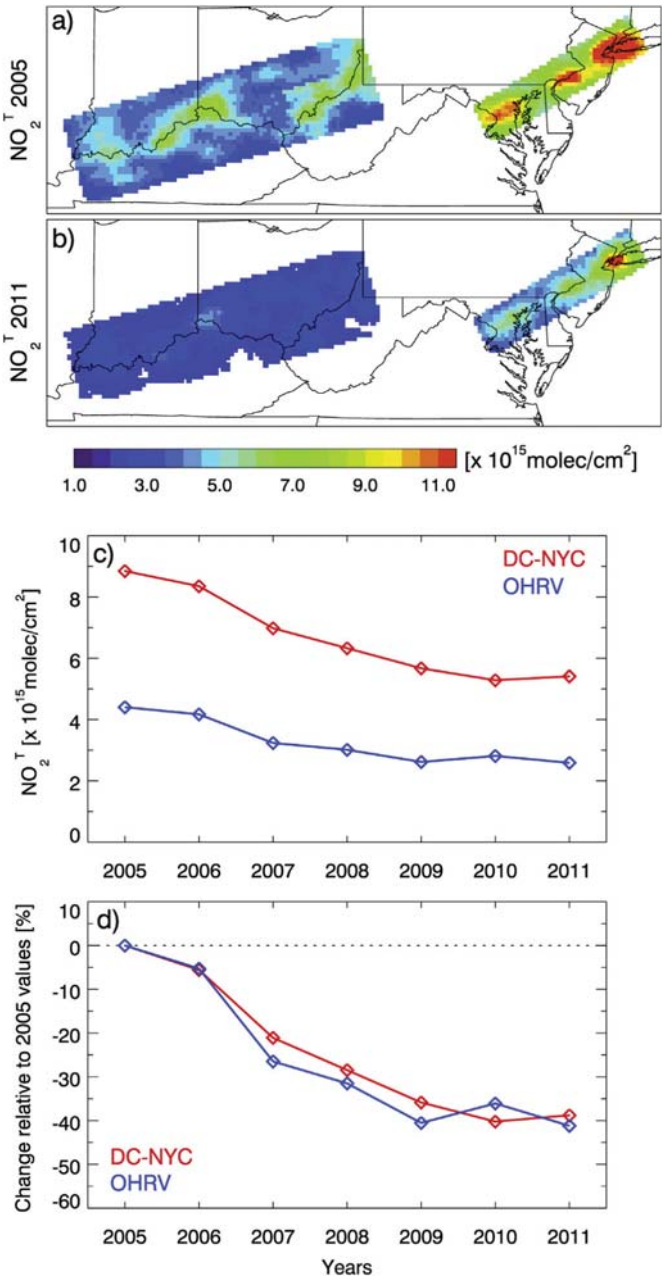

Fig. 5. Annual mean NO_2^T ($\times$ 10^{15} molecules cm^{-2}) for a) 2005 and b) 2011 for two regions: the Ohio River Valley (OHRV), which has a high concentration of power plants, and the densely populated Northeast Corridor (DC-NYC). Data $<2 \times 10^{15}$ molecules cm^{-2}, which have low SNRs, are shown as white in these two regions. The c) absolute and d) percent changes in the mean data for the two regions relative to levels in 2005.

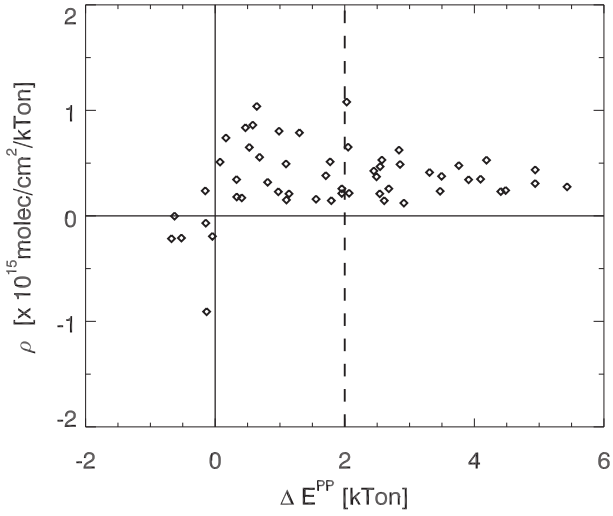

Fig. 6. ρ ($\times 10^{15}$ molec (cm^2 kTon)$^{-1}$) versus ΔE^{PP} (kTon) for the individual facilities. The vertical dashed line separates ΔE^{PP} into two categories: $\Delta E^{PP} > 2$ kTon, $\Delta E^{PP} < 2$ kTon.

may decide to exclude the winter season from the analysis because of issues associated with NO_x lifetime and statistical significance as discussed above. We repeated our analysis, excluding the winter season, and found that the conclusions of our study remain unchanged. The correlations of ΔE^{PP} and ΔNO_2^T changed modestly for most facilities, though we did not find an improvement in the scatter observed in Fig. 3 as indicated by the correlation statistic (r). r^2 for the northern US decreased from 0.18 to 0.07 and remained the same for the southern US. Based on the discussion in this section, it is important to understand that the value of ρ will depend on the choice of months used in the analysis, particularly in regions with seasonal variation in the NO_x lifetime.

3.2.6. Variations in regional NO_2 levels (ΔNO_2^0)

Annual mean surface concentrations of NO_2 decreased 33% nationally between 2001 and 2010 (EPA, 2012), primarily from decreases in emissions from fuel combustion in electrical utilities and vehicles (e.g., McDonald et al., 2012). From 2005 to 2011, the combined NO_x emissions reduction from electrical utilities and vehicles was about 37% (http://www.epa.gov/ttn/chief/trends/index.html) with two-thirds of the decrease being attributed to the reduction in the mobile source. The OMI data confirm that regional NO_2 levels decreased substantially in many areas of the US during our study period (e.g., Russell et al., 2012). Fig. 4 shows the percent change relative to 2005 of EPA's Air Quality Monitoring System (AQS; http://www.epa.gov/ttn/airs/airsaqs/) NO_2 data and the corresponding OMI data above the AQS stations. The data are averaged over the whole US and over four quadrants. The reductions by 2009 range from 20 to 30% for the AQS sites as grouped in the quadrants, but 35–40% for OMI data; the northwest quadrant is an outlier. However, the overall shapes of the trends in both datasets are similar. The discrepancy in the magnitudes of the trends of the AQS and OMI data may occur as the OMI detects changes in NO_2 throughout the whole troposphere, while monitors at the AQS sites sample near-surface air. Thus, the OMI detects the reductions in NO_2 associated with both mobile and power plant sources, while the AQS surface monitors preferentially sample reductions in mobile sources as power plant plumes are located aloft predominately.

Though the chemical lifetime of NO_x is relatively short, NO_x emissions upwind influence NO_2 columns downwind (e.g., Turner et al., 2012), which can lead to elevated regional NO_2 levels (As discussed in Section 2.2 for our analysis, we selected facilities least affected by other sources within a 0.4° longitude $\times$ 0.4° latitude area around the facility (i.e., $f_{power} > 0.90$)). Over our study period, some of the largest changes in regional levels occurred in the heavily populated region extending from Washington, DC to New York City (i.e., the Northeast Corridor), and the industrialized Ohio River Valley, where eight of the power plants selected for this study are located; the Chalk Point facility (ID #20) is the only facility that met our criterion (i.e., $f_{power} > 0.90$) for selection in the Northeast Corridor. Fig. 5 shows that regional NO_2 levels decreased by 30–40% from 2005 to 2011 in both of these regions, though the absolute decrease was much higher in the Northeast Corridor. Most of the power plants in Table 1 are located in areas with lower regional NO_2 levels in 2005 than in the Northeast Corridor and Ohio River Valley.

Fig. 6 shows the relationship between ΔE^{PP} and ρ. For power plants with $\Delta E^{PP} > 2$ kTon, ΔE^{PP} is generally large relative to the change in the regional NO_2 level. ρ's for these facilities are between 0.12 and 0.62 with a mean of 0.36. For facilities with $\Delta E^{PP} < 2$ kTon, there is a wider range of ρ's (i.e., between −0.91 and 1.08), indicating that a change in the regional NO_2 level, if large, can influence ρ in a non-negligible way. We attempted to find a method for removing the influence of a change in the regional NO_2 level in a general way applicable to all facilities. However, we found that the change in the regional NO_2 level can vary widely (e.g., with meteorological variability), requiring careful processing of the data for each facility. As an example, NO_2^T's were high at the nearby facilities of White Bluff (ID #46) and Dolet Hills (ID # 25) in the winters of 2009–10 and 2010–11 (Figure S1), which we found to be caused by stagnant meteorological conditions that allowed regional NO_2 levels to build.

4. Summary

We conclude that it is practical to use OMI NO_2 tropospheric column data to assess changes of emissions from power plants that are associated with the implementation of emission control devices (ECDs), though careful interpretation of the data is necessary. We showed that there is a clear response for OMI NO_2 data to NO_x emission reductions from power plants associated with the implementation of ECDs on both monthly and annual timescales. This response is scalar for all intents and purposes, whether the reduction is rapid or incremental over several years. However, the response is variable among the power plants, even those with the greatest absolute decrease in emissions. We discussed some of the causes of this variability, which include the magnitude of a facility's NO_x emissions, seasonal variation of the NO_x lifetime, proximity to urban areas, changes in the regional NO_2 levels, lack of statistical significance, and retrieval issues. Ideally, one should use a CTM to account for several of these causes of variability, though this would limit the practical application of space-based data for air quality purposes because of computational expense. However, we show that this step is not necessary if the change in the facility's NO_x emissions is large.

Using space-based NO_2 columns to assess changes in power plant NO_x emissions will likely become more quantitative as the OMI retrieval procedure continues to evolve, such as through the use of improved and finely-resolved information of surface parameters. In addition, two planned sensors promise enhanced capabilities as compared to OMI: i) the European Space Agency Tropospheric Ozone Monitoring Instrument (TROPOMI; http://www.knmi.nl/samenw/tropomi/Instrument/), an OMI follow-on instrument with finer horizontal resolution, and ii) the NASA Tropospheric Emissions: Monitoring of Pollution (TEMPO; http://science.nasa.gov/missions/tempo/) instrument, an OMI-like instrument that will be in geostationary orbit, collecting data throughout the day as opposed to one overpass per day as with OMI.

Many of the facilities included in our study were already using ECDs during the ozone season before the start of the OMI data record. A next step would be to repeat our analysis over the SCIAMACHY, GOME, and GOME-2 records, similar to the study of Lu and Streets (2012), extending the period of study to 1996. The limitation of this approach is that the horizontal resolutions of data from these instruments are coarser than OMI data, which would make it more difficult to isolate the signal of individual facilities from signals of other nearby sources.

Acknowledgments

This work was funded by the NASA Air Quality Applied Sciences Team (AQAST) program. We acknowledge the free use of 1) tropospheric NO_2 column data from the Aura OMI, 2) NO_x emissions data from the US EPA, and 3) EDGAR data, which is maintained as a joint project of the European Commission Joint Research Centre (JRC) and the Netherlands Environmental Assessment Agency (PBL).

Appendix A. Supplementary data

Supplementary data related to this article can be found at http://dx.doi.org/10.1016/j.atmosenv.2013.08.068.

References

Beirle, S., Boersma, K., Platt, U., Lawrence, M., Wagner, T., 2011. Megacity emissions lifetimes of nitrogen oxides probed from space. Science. http://dx.doi.org/10.1126/science.1207824.

Boersma, K., Eskes, H., Brinksma, E., 2004. Error analysis for tropospheric NO_2 retrieval from space. J. Geophys. Res. 109 (D04311). http://dx.doi.org/10.1029/2003JD003962.

Boersma, K., Eskes, H., Dirksen, R., van der, A.R., Veefkind, J., Stammes, P., Huijnen, V., Kleipool, Q., Sneep, M., Claas, J., Leitão, J., Richter, A., Zhou, Y., Brunner, D., 2011. An improved tropospheric NO_2 column retrieval algorithm for the Ozone Monitoring Instrument. Atmos. Measur. Tech. 4. http://dx.doi.org/10.5194/amt-4-1905-2011.

Bucsela, E.J., Krotkov, N.A., Celarier, E.A., Lamsal, L.N., Swartz, W.H., Bhartia, P.K., Boersma, K.F., Veefkind, J.P., Gleason, J.F., Pickering, K.E., 2013. A new algorithm for retrieval of vertical column NO_2 from nadir-viewing satellite instruments. Atmos. Measur. Tech. Discus. 6, 1361–1407.

Dallmann, T., Harley, R., 2010. Evaluation of mobile source emission trends in the United States. J. Geophys. Res. 115 (D14305). http://dx.doi.org/10.1029/2010JD013862.

Dobber, M., Braak, R., 2010. Known Instrumental Effects that Affect the OML1B Product of the Ozone Monitoring Instrument on EOS Aura. Last Update: 17 December 2010 http://disc.sci.gsfc.nasa.gov/Aura/data-holdings/OMI/documents/v003/known_instrumental_effects_l1b_data_omi_v6.pdf.

EPA, 2012. Our Nation's Air: Status and Trends Through 2010. Environmental Protection Agency. EPA-454/R-12–001.

Kaynak, B., Hu, Y., Martin, R., Sioris, C., Russell, A., 2009. Comparison of weekly cycle of NO_2 satellite retrievals NO_x emission inventories for the continental United States. J. Geophys. Res. 114 (D05302). http://dx.doi.org/10.1029/2008JD010714.

Kim, S.-W., Heckel, A., McKeen, S., Frost, G., Hsie, E.-Y., Trainer, M., Richter, A., Burrows, J., Peckham, S., Grell, G., 2006. Satellite-observed U.S. power plant NO_x emission reductions their impact on air quality. Geophys. Res. Lett. 33 (L22812). http://dx.doi.org/10.1029/2006GL027749.

Kim, S.-W., Heckel, A., Frost, G., Richter, A., Gleason, J., Burrows, J.P., McKeen, S., Hsie, E.-Y., Granier, C., Trainer, M., 2009. NO_2 columns in the western United States observed from space simulated by a regional chemistry model their implications for NO_x emissions. J. Geophys. Res. 114 (D11301). http://dx.doi.org/10.1029/2008JD011343.

Lamsal, L., Martin, R., van Donkelaar, A., Celarier, E., Bucsela, E., Boersma, K., Dirksen, R., Luo, C., Wang, Y., 2010. Indirect validation of tropospheric nitrogen dioxide retrieved from the OMI satellite instrument: insight into the seasonal variation of nitrogen oxides at northern midlatitudes. J. Geophys. Res. 115 (D05302). http://dx.doi.org/10.1029/2009JD013351.

Lamsal, L., Martin, R., Padmanabhan, A., van Donkelaar, A., Zhang, Q., Sioris, C., Chance, K., Kurosu, T., Newchurch, M., 2011. Application of satellite observations for timely updates to global anthropogenic NO_x emission inventories. Geophys. Res. Lett. 38 (L05810). http://dx.doi.org/10.1029/2010GL046476.

Lamsal, et al., 2013. Evaluation of Improved Operational Standard Tropospheric NO_2 Retrievals from Ozone Monitoring Instrument Using in Situ Surface-based NO_2 Observations. in preparation).

Lu, Z., Streets, D., 2012. Increase in NO_x emissions from Indian thermal power plants during 1996–2010: unit-based inventories multisatellite observations. Environ. Sci. Technol. 46, 7463–7470. http://dx.doi.org/10.1021/es300831w.

Levelt, P.F., van den Oord, G.H.J., Dobber, M.R., Mälkki, A., Visser, H., de Vries, J., Stammes, P., Lundell, J.O.V., Saari, H., 2006. The Ozone Monitoring Instrument. Trans. Geosci. Remote Sens. 44, 1093–1101. http://dx.doi.org/10.1109/TGRS.2006.872333.

Martin, R., Jacob, D., Chance, K., Kurosu, T., Palmer, P., Evans, M., 2003. Global inventory of nitrogen oxide emissions constrained by space-based observations of NO_2 columns. J. Geophys. Res. 108, 4537. http://dx.doi.org/10.1029/2003JD003453.

McDonald, B., Dallmann, T., Martin, E., Harley, R., 2012. Long-term trends in nitrogen oxide emissions from motor vehicles at national, state, air basin scales. J. Geophys. Res. 117 (D00V18). http://dx.doi.org/10.1029/2012JD018304.

Palmer, P., Jacob, D., Chance, K., Martin, R., Spurr, R., Kurosu, T., Bey, I., Yantosca, R., Fiore, A., Li, Q., 2001. Air mass factor formulation for spectroscopic measurements from satellites: application to formaldehyde retrievals from the Global Ozone Monitoring experiment. J. Geophys. Res. 106 (D13), 14539–14550 doi: 0148-0227/01/2000JD900772.

Platt, U., 1994. Differential Optical Absorption Spectroscopy (DOAS). In: Air Monitoring by Spectroscopic Techniques. John Wiley, New York, pp. 27–84.

Russell, A., Valin, L., Cohen, R., 2012. Trends in OMI NO_2 observations over the US: effects of emission control technology the economic recession. Atmos. Chem. Phys. 12, 12197–12209. http://dx.doi.org/10.5194/acp-12-12197-2012.

Stavrakou, T., Müller, J.-F., Boersma, K., De Smedt, I., van der, A.R., 2008. Assessing the distribution growth rates of NO_x emission sources by inverting a 10-year record of NO_2 satellite columns. Geophys. Res. Lett. 35 (L10801). http://dx.doi.org/10.1029/2008GL033521.

Streets, D., Canty, T., Carmichael, G., de Foy, B., Dickerson, R., Duncan, B., Edwards, D., Haynes, J., Henze, D., Houyoux, M., Jacob, D., Krotkov, N., Lamsal, L., Liu, Y., Lu, Z., Martin, R., Pfister, G., Pinder, R., Salawitch, R., Wecht, K., 2013. Emissions estimation from satellite retrievals: a review of current capability. Atmos. Environ.. http://dx.doi.org/10.1016/j.atmosenv.2013.05.051.

Turner, A., Henze, D., Martin, R., Hakami, A., 2012. The spatial extent of source influences on modeled column concentrations of short-lived species. Geophys. Res. Lett. 39 (L12806). http://dx.doi.org/10.1029/2012GL051832.

Walter, D., Heue, K.-P., Rauthe-Schoch, A., Brenninkmeijer, C., Lamsal, L., Krotkov, N., Platt, U., 2012. Flux calculation using CARIBIC DOAS aircraft measurements: SO_2 emission of Norilsk. J. Geophys. Res. 117 (D11305). http://dx.doi.org/10.1029/2011JD017335.

Zhou, Y., Brunner, D., Boersma, K., Dirksen, R., Wang, P., 2009. An improved tropospheric NO_2 retrieval for satellite observations in the vicinity of mountainous terrain. Atmos. Measur. Tech. 2, 401–416.

Zhou, Y., Brunner, D., Hueglin, C., Henne, S., Staehelin, J., 2012. Changes in OMI tropospheric NO_2 columns over Europe from 2004 to 2009 the influence of meteorological variability. Atmos. Environ. 46. http://dx.doi.org/10.1016/j.atmosenv.2011.09.024.